PHYSICAL REVIEW C VOLUME 17, NUMBER 1 JANUARY 1978

Nuclear level density with schematic forces

B. C. Smith,* F. N. Choudhury,† and S. Das Gupta
Physics Department, McGill University, Montreal, Canada
(Received 8 July 1977)

For a system of fermions interacting via a pure pairing force, exact level densities are obtained in a semirealistic model space. The results are transmitted through graphs and tables so that they are readily available for comparison with various approximate methods. A fairly detailed comparison with a particular approximate method using the grand partition function is also made. The consequences of adding the quadrupole force to the Hamiltonian are discussed. Variational calculations done in the specific case of Sn isotopes suggest that although these nuclei are spherical in the ground state (zero temperature), it is possible that they prefer deformation at finite but low temperature. This can lead to very large changes in the calculated values of level densities.

[NUCLEAR STRUCTURE ^{116}Sn, ^{117}Sn; calculated level density using quasispin formalism, grand partition method, and pairing-plus-quadrupole model at finite temperature.]

I. INTRODUCTION

Nuclear level density data are available mostly at neutron separation energies. The motivation for doing level density calculations at these energies is to ascertain if the parameters that give a reasonable description of very low energy spectra can also reproduce the level density data.

At the present time, most level density calculations[1-5] employ realistic single particle levels. Thus shell effects are already built into the calculations. Often the only residual interaction employed is the pairing force which is solved in an approximate way. Usually an approximate grand partition function is constructed[1-4] from which the level density is obtained by Laplace inversion, although different approximations[5] have also been made.

In doing similar calculations in the Sn isotopes[6] we have felt the need for some exact calculations against which approximate calculations could be compared. The present work was initially planned with this in mind. The model space for which exact calculations are to be done must be semirealistic. Thus we have avoided level density calculations involving fermions in a single j shell. On the other hand, a completely realistic valence space is too large to handle exactly. We have, therefore, limited ourselves to a moderately large space and allowed fermions to interact by a pairing force. Exact level density calculations for even-A and odd-A systems were done in this space. These results are transmitted through graphs and tables such that they are readily available for studying the suitability of any approximate method.

The second motivation for this paper arose as a byproduct of this study above. Having established the bounds for approximate calculations, we realized that it is not possible to achieve agreement with the experimental data in Sn isotopes using the pairing force as the only residual interaction. If we use realistic single particle energies and a pairing force which reproduces odd-even mass differences, then the calculated level densities are small by a factor of 20 or worse. Discrepancies of the order of 100 for these isotopes have been mentioned in the literature before.[3] We ourselves have done a level density calculation[6] in this region with Lee-Kahana-Scott[7] matrix elements; the results do not change appreciably.

One solution to this dilemma is the following interesting possibility. As is well established, the Sn isotopes are spherical in the ground state. All calculations mentioned above assume that they remain so at higher excitation energy. Suppose, however, that a large number of excited intrinsic states at ≈8 MeV in these nuclei are deformed. Then rotational states built upon these deformed intrinsic states will lead to a large increase in level density. Such an increase can be as high as a factor of 40 (see Refs. 3 and 4) in the well deformed region. A variational calculation done in this paper is strongly indicative of the possibility that at excitation energies of the order of 8 MeV, the Sn isotopes are, in a statistical sense, deformed. We investigate this by adding the quadrupole force to the pairing Hamiltonian and calculating the energy surface against deformation at zero temperature (ground state) as well as at finite temperature (excited states). At zero temperature, the shape is spherical; at finite but still low tem-

TABLE I. Neutron shell model energies for exact calculation in model space.

Orbital	Energy (MeV)
$1d_{5/2}$	0
$0g_{7/2}$	0.8
$2s_{1/2}$	1.3
$0h_{11/2}$	2.50
$1d_{3/2}$	2.80

perature, the pairing effect is weakened and the quadrupole force takes over, giving preference to a deformed shape over the spherical shape.

II. EXACT CALCULATIONS IN A MODEL SPACE

We consider ^{116}Sn, ^{117}Sn, and ^{120}Sn. These are regarded as 16, 17, and 20 neutrons in the $1d_{5/2}$, $0g_{7/2}$, $2s_{1/2}$, $0h_{11/2}$, and $1d_{3/2}$ shells. The single particle energies are taken from Kisslinger and Sorensen[8] and are listed in Table I. The pairing force strength is $g = 23/A$ MeV. The exact diagonalizations were done using Kerman's quasispin formalism.[9] In spite of the simplification that this formalism provides, some of the matrices are quite large. The largest matrix in the case of ^{116}Sn was 110×110.

The results of matrix diagonalization are shown in the form of histograms in Figs. 1 and 2. Exact level densities obtained from a pure pairing force exhibit significant fluctuations. Some of these fluctuations are not real but rather result from the simple nature of the pairing force which leads to many degeneracies. It is desirable to smooth these fluctuations in order to compare with results from approximate methods which provide a smoothed density. We smooth the exact level[6] density by using the saddle-point method. This requires the following steps. From the exact eigenvalues one can obtain

$$Z_c(\beta) = \sum e^{-\beta E_i} .$$

The exact density is related to Z_c by

$$\rho(E) = \frac{1}{2\pi i} \int_{-i\infty}^{i\infty} Z_c(\beta) e^{\beta E} d\beta .$$

The integral is evaluated by the saddle-point method and leads to

$$\rho(E) = \exp[\ln Z_c(\beta_0) + \beta_0 E] / [2\pi(\langle E^2 \rangle - E^2)]^{1/2} ,$$

where

$$E = \sum E_i e^{-\beta_0 E_i} / Z_c(\beta_0) ,$$

$$\langle E^2 \rangle = \sum E_i^2 e^{-\beta E_i} / Z_c(\beta_0) .$$

In the present context, the main feature of the saddle-point method is that it converts a discrete density into a smooth one.

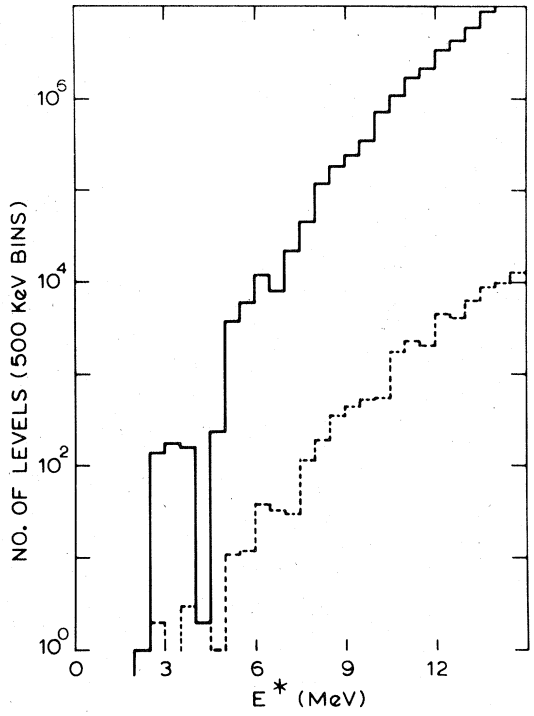

FIG. 1. Histogram of energy levels for ^{116}Sn. The solid line represents the state density including a sum over states of both parities and all spins and all magnetic substates (yielding a factor of $2I+1$). The dashed line represents the level density. It is a sum over the levels of spin 0^+ and 1^+ with only one magnetic substate included for each spin.

The smoothed densities obtained from the exact calculations are given in Table II. In all subsequent sections, these smoothed densities are referred to as exact densities. We provide numerical values of $\omega(E)$ and $\rho(E, I, \pi)$ where

$$\omega(E) = \sum_I (2I+1)\rho(E, I)$$

$$= \sum_I (2I+1)[\rho(E, I, +) + \rho(E, I, -)] .$$

In many approximate calculations, $\omega(E)$ is obtained first and $\rho(E, I, \pi)$ is obtained subsequently. Experimental results are usually for selective values of I with definite parity.

III. APPROXIMATE METHOD BASED ON THE GRAND PARTITION FUNCTION APPROACH

If the exact grand partition function

$$Z(\alpha, \beta) = \sum_{N,i} e^{\alpha N} e^{-\beta E_i(N)}$$

$$= \sum e^{\beta[\lambda N - E_i(N)]} \qquad (1)$$

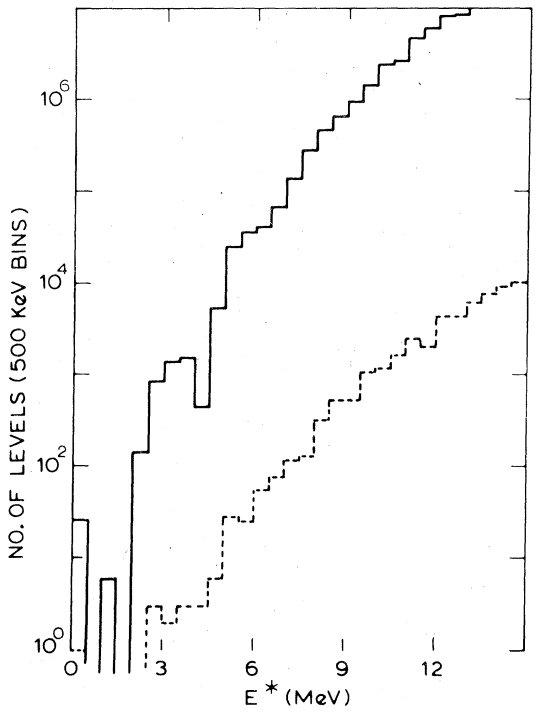

FIG. 2. Histogram of energy levels for ^{117}Sn. The solid line represents the state density as described in the caption to Fig. 1. The dashed line represents the level density for spin $\frac{1}{2}^+$.

is known, then the exact expression for state density of N particles is given by

$$\omega_N(E)=\frac{1}{(2\pi i)^2}\int\int_{-i\infty}^{i\infty} Z(\alpha,\beta)e^{-\alpha N}e^{\beta E}d\alpha\, d\beta. \qquad (2)$$

The saddle-point approximation for the integral leads to

$$\omega_N(E)=e^S/[2\pi(D_{\alpha\alpha}D_{\beta\beta}-D_{\alpha\beta}{}^2)^{1/2}], \qquad (3)$$

where the entropy S is

$$S=\ln Z(\alpha_0,\beta_0)-\alpha_0 N+\beta_0 E \qquad (4)$$

and the constants α_0, β_0 are so chosen that

$$\left.\frac{\partial \ln Z}{\partial \alpha}\right|_{\alpha_0,\beta_0}=N, \qquad (5)$$

$$\left.\frac{\partial \ln Z}{\partial \beta}\right|_{\alpha_0,\beta_0}=-E. \qquad (6)$$

The quantities $D_{\alpha\alpha}$, $D_{\beta\beta}$, and $D_{\alpha\beta}$ are second derivatives:

$$D_{\alpha\alpha}=\left.\frac{\partial^2 \ln Z}{\partial \alpha^2}\right|_{\alpha_0,\beta_0}, \qquad (7)$$

$$D_{\beta\beta}=\left.\frac{\partial^2 \ln Z}{\partial \beta^2}\right|_{\alpha_0,\beta_0}, \qquad (8)$$

$$D_{\alpha\beta}=\left.\frac{\partial^2 \ln Z}{\partial \alpha\,\partial \beta}\right|_{\alpha_0,\beta_0}. \qquad (9)$$

Provided the residual force is the pairing interaction, an approximate grand partition function can be readily obtained and the various quantities appearing on the right-hand side of Eq. (3) can be readily obtained. The method has recently been extended to include more general interaction.[6] For completeness, we write down the equations that need to be solved for a pure pairing force. For a given temperature $\tau(=1/\beta)$ one solves

$$N=\sum \Omega_j\left[1-\frac{\epsilon_j-\lambda}{E_j}(1-2f_j)\right], \qquad (10)$$

$$\frac{2}{g}=\sum \Omega_j\frac{1}{E_j}(1-2f_j). \qquad (11)$$

In the above, ϵ_j are shell model single particle energies, $\Omega_j=(j+\frac{1}{2})$ and

TABLE II. The smoothed state density $\omega(E)$ and smoothed level density $\rho(E,I,\pi)$ for ^{116}Sn and ^{117}Sn resulting from an exact calculation in the model space. Each density must be multiplied by 10 exponentiated by the number given in brackets.

Excitation energy (MeV)	^{116}Sn $\omega(E)$ (MeV^{-1})	^{116}Sn $\rho(E,0,+)+\rho(E,1,+)$ (MeV^{-1})	^{117}Sn $\omega(E)$ (MeV^{-1})	^{117}Sn $\rho(E,\frac{1}{2},+)$ (MeV^{-1})
5	3(3)	...	2(4)	...
6	1.3(4)	...	7(4)	...
7	4.7(4)	1(2)	2.3(5)	2(2)
8	1.4(5)	3(2)	6.5(5)	4(2)
9	4.2(5)	6(2)	1.6(6)	9(2)
10	1.1(6)	1(3)	3.7(6)	2(3)
11	2.6(6)	3(3)	7.5(6)	4(3)
12	5.4(6)	6(3)	1.4(7)	7(3)
13	1.0(7)	1.1(4)	2.3(7)	1.0(4)
14	1.9(7)	1.8(4)	3.4(7)	1.6(4)
15	3.0(7)	3(4)	4.8(7)	2.1(4)

$$E_j = [(\epsilon_j - \lambda)^2 + \Delta^2]^{1/2},$$

$$f_j = (1 + e^{\beta E_j})^{-1}.$$

Δ is the energy gap which is largest at zero temperature and decreases with increasing temperature. Above the critical temperature, Eq. (11) cannot be satisfied and the problem reduces to that of noninteracting fermions. The explicit expressions for the various quantities appearing on the right-hand side of Eq. (3) can be found in previous work.[1-4]

To obtain $\rho(E,I)$ we use

$$\rho(E,I) = \rho(E,M=I) - \rho(E,M=I+1),$$

$$\rho(E,M) = (2\pi\sigma^2)^{-1/2}\omega(E)\exp(-M^2/2\sigma^2),$$

where

$$\sigma^2 = \sum \left(2 \sum_{m=1/2}^{j} m^2\right) f_j(1-f_j).$$

The quantity σ^2 is called the spin cutoff factor. Finally it is assumed that $\rho(E,I,+) = \frac{1}{2}\rho(E,I)$.

The level densities derived from this approximate method are compared with exact densities in Figs. 3 and 4. The approximate method is correct to within a factor of 2. One feature of the approximate calculation is that it underestimates the level density below the critical temperature and overestimates it above it. The level density obtained from the approximate calculation has an abrupt rise at the critical temperature. This is associated with a sudden decrease in the value of $D_{\beta\beta}$ [Eqs. (3) and (8)] at the critical temperature.

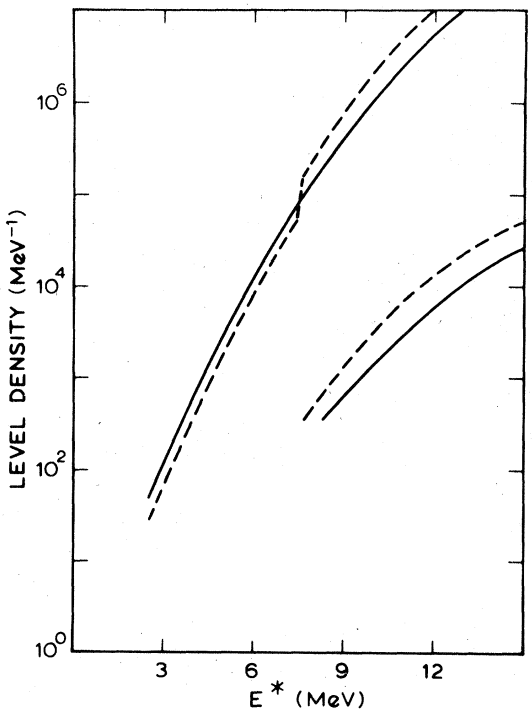

FIG. 3. State density and level density for ^{116}Sn. The solid lines represent the densities obtained by smoothing the exact results by the saddle-point method. They correspond to the histograms in Fig. 1. The dashed lines represent the approximate densities obtained from the grand partition function method.

IV. THE METHOD OF MOMENTS

This method was pioneered by French and collaborators.[10] Consider N fermions restricted to M single particle states $[M = \sum(2j_a + 1)]$. Then, to lowest order,

$$\omega_N(E) = (2\pi F^2)^{-1/2} d(N) \exp[-(E-\bar{E})^2/2F^2]. \quad (12)$$

Here

$$d(N) = \binom{M}{N}, \quad (13)$$

$$\bar{E} = \frac{1}{d}\sum_i \langle N,i|H|N,i\rangle, \quad (14)$$

$$F^2 = \langle E^2\rangle - \bar{E}^2, \quad (15)$$

$$\langle E^2\rangle = \frac{1}{d}\sum_i \langle N,i|H^2|N,i\rangle. \quad (16)$$

In Eqs. (14) and (16), the index i runs over all possible states of the N particle system in the re-

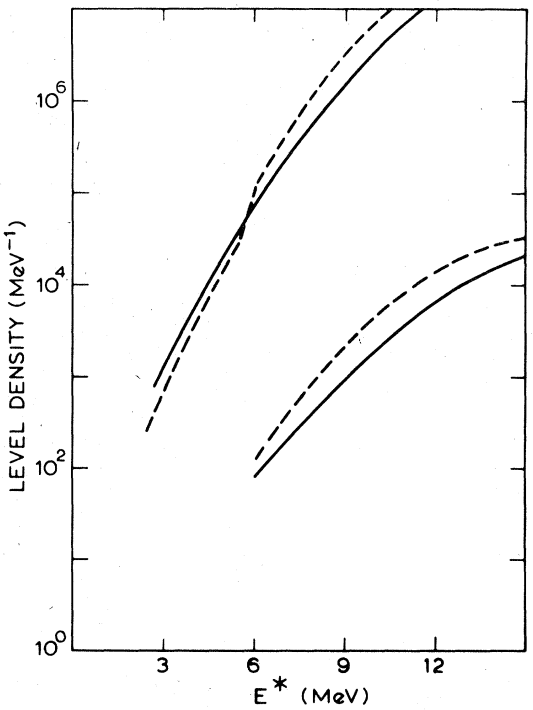

FIG. 4. State density and level density for ^{117}Sn as described in caption to Fig. 3.

stricted space. An equation similar to Eq. (12) above can be written down for $\rho(E,I,\pi)$ or for a sum of $\rho(E,I,\pi)$ with appropriate changes in d, $\bar{E}$, and E^2. Equation (12) is the first term of a Gram-Charlier series[10] and can also be obtained[11] from standard techniques of statistical mechanics.

The method was compared with exact calculation in the following way. We assume that $\rho(E) \equiv \rho(E,0,+)+\rho(E,1,+)$ (this is the experimentally measured quantity in ^{120}Sn) is described by a Gaussian with parameters defined by appropriate modifications of Eqs. (13)–(16). It is well known[12] that the pairing force produces some skewness in the distribution which is not contained in the lowest order expression of Eq. (12). Nonetheless, the Gaussian distribution fits the exact density moderately well. The real problem lies in trying to rewrite Eq. (12) in terms of $\rho(E_{\rm exc})$ where $E_{\rm exc}$ is the excitation energy. This is necessary for comparing with experiment. If we decide to approximate the ground state energy[12] by E_0 where E_0 satisfies

$$\int_{-\infty}^{E_0} \rho(E)dE = \tfrac{1}{2}$$

and use Eq. (12) to calculate $\rho(E_{\rm exc})$, large errors are obtained. For example, $\rho(E_{\rm exc})$ overestimates the exact density by a factor of 7 in ^{120}Sn at 9 MeV excitation.

V. COMPARISON WITH EXPERIMENTAL DATA

The calculations described in the previous sections were performed to test the validity of the various approximations. If we now compare our exact model space calculation with experimental data, we find that we underestimate the experimental density of states by about a factor of 25 in each of the nuclei studied (^{116}Sn, ^{117}Sn, and ^{120}Sn). The first remedy that comes to mind is to increase the valence space. In this increased space (see Table III) exact calculations are not possible. We use the approximate grand partition method of Sec. III since it was a reasonable approximation in the model space. When increasing the valence space, the value of the pairing force constant g has to be decreased such that the gap Δ at zero temperature remains unchanged. The gap Δ essentially gives odd-even mass differences. The results of the larger space calculations are shown in Fig. 5. Theoretical calculations still underestimate experimental results by unacceptable factors. It is possible to obtain the correct experimental data by further reducing the value of g by more than 20%. However, this reduces the value of Δ to unacceptably low values. There is another possible solution to our dilemma.

It is well known that the major features of the residual interaction can be simulated by two forces—the pairing force and the quadrupole force. So long as the nucleus remains spherical, the quadrupole force makes no contribution to the energy of the system. The deformation of a nucleus is the result of two competing effects: the pairing force, which tends to make nuclei spherical, and the quadrupole force, which favors deformation. In Sn isotopes, at zero temperature the pairing force dominates and a spherical shape is favored. However, as mentioned before (Sec. III), at finite temperatures the effect of the pairing force is reduced and Δ drops in value. But, if the pairing effect is reduced, what keeps the nucleus from deforming? Of course, finite temperature tends to wash out the effects of the quadrupole force as well; however, it is a matter of differential effects that one is studying. Provided nuclei do favor deformation, it is clear that a different formalism should be used to calculate level density at the appropriate excitation energy.

Quite apart from the question of level density, the possibility of deformation at finite temperature in a nucleus which is spherical in its ground state is interesting in itself. The effect of the quadrupole force on the level density was investigated by Kanestrom[13] using the SU_3 scheme. However, the pairing force and the one-body spin-orbit force was not taken into account. Hillman[14] considered approximate solutions of the pairing force problem in the Nilsson scheme of single particle levels. That calculation we believe is much harder to execute compared to what follows in the next section.

TABLE III. Shell model energies used in full space calculations. These energies were calculated for a spherical Woods-Saxon potential well (N. B. de Takacsy, private communication). The energy scale for the neutrons has been shifted so that the $1d_{5/2}$ orbital has zero energy. The energies identified by an asterisk are the same as those given in Table I.

Orbital	Energy (MeV) Proton	Neutron
$1p_{1/2}$	−9.6370	···
$1p_{3/2}$	−10.7590	···
$0f_{5/2}$	−11.2241	···
$0f_{7/2}$	−15.6952	···
$2s_{1/2}$	−0.6689	1.3*
$1d_{3/2}$	−0.7496	2.8*
$1d_{5/2}$	−2.5082	0.0*
$1d_{7/2}$	−2.4893	0.8*
$0g_{9/2}$	−7.7014	−4.6600
$2p_{1/2}$	···	9.6320
$2p_{3/2}$	···	8.9192
$1f_{5/2}$	···	10.2434
$1f_{7/2}$	···	7.6839
$0h_{9/2}$	···	10.2813
$0h_{11/2}$	···	2.5*

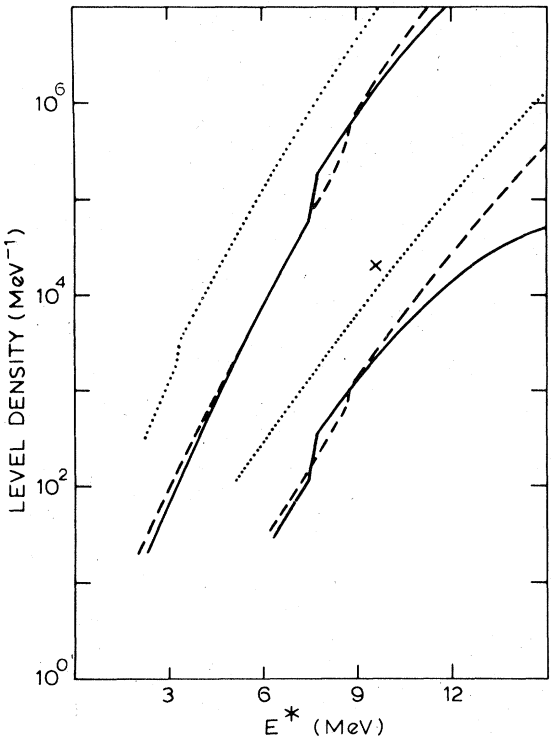

FIG. 5. State density and level density for ^{116}Sn resulting from the grand partition function method. The solid lines are the same as the dotted lines in Fig. 3 and result from a calculation in the semirealistic space defined in Table I. The dashed lines give the results for the full space (Table III) with g suitably modified to keep the correct Δ. The dotted lines are obtained by repeating the full space calculation but with the pairing force reduced by 20%. This gives closer agreement with the experimental value indicated by an $\times$. Unfortunately this reduces the pairing gap Δ from 1.234 MeV to the unrealistically low value of 0.714 MeV.

VI. PAIRING PLUS QUADRUPOLE FORCE AT FINITE TEMPERATURE

We take the quadrupole force to be

$$V(1,2) = -\chi r_1^2 r_2^2 \sum_\mu Y_{2\mu}(1) Y_{2\mu}^*(2) .$$

The other part of the residual interaction is the pairing force. At zero temperature the energy vs axially symmetric deformation can be studied[15] by the following procedure.

(1) Diagonalize the one-body Hamiltonian

$$H = H_0 - D r^2 Y_{20} \tag{17}$$

to obtain eigenvalues ϵ_k. Here H_0 is the shell model part and D is a parameter. If we equate $D = m\omega^2\beta_2$, where ω is the appropriate oscillator frequency, then β_2 is closely related to the quadrupole deformation parameter of the Nilsson model.

(2) The pairing force problem is now solved on these deformed orbitals. This means one solves

$$N = \sum_{k>0} \left(1 - \frac{\epsilon_k - \lambda}{E_k}\right), \tag{18}$$

$$\frac{2}{g} = \sum_{k>0} \frac{1}{E_k}, \tag{19}$$

where $E_k = [(\epsilon_k - \lambda)^2 + \Delta^2]^{1/2}$. The energy of the system as a function of deformation is given by

$$E(\beta_2) = \sum_{k>0} (H_0)_{kk} \left(1 - \frac{\epsilon_k - \lambda}{E_k}\right) - \tfrac{1}{2}\chi Q_0^2 - \Delta^2/g , \tag{20}$$

where

$$Q_0 = \sum_{k>0} \langle k | r^2 Y_{20} | k \rangle \left(1 - \frac{\epsilon_k - \lambda}{E_k}\right). \tag{21}$$

An extremum in energy is obtained whenever $D = \chi Q_0$.

The generalization of this procedure to a given finite temperature $\tau (= 1/\beta)$ leads to the following steps.

(1′) Same as (1).

(2′) One solves

$$N = \sum_{k>0} \left[1 - \frac{\epsilon_k - \lambda}{E_k}(1 - 2f_k)\right], \tag{22}$$

$$\frac{2}{g} = \sum_{k>0} \frac{1}{E_k}(1 - 2f_k) . \tag{23}$$

Here, as before, $E_k = [(\epsilon_k - \lambda)^2 + \Delta^2]^{1/2}$ and $f_k = 1/(1 + e^{\beta E_k})$. The energy of the system as a function of deformation is given by

$$E(\beta_2) = \sum_{k>0} (H_0)_{kk} \left[1 - \frac{\epsilon_k - \lambda}{E_k}(1 - 2f_k)\right] - \tfrac{1}{2}\chi Q_0^2 - \Delta^2/g , \tag{24}$$

where

$$Q_0 = \sum_{k>0} \langle k | r^2 Y_{20} | k \rangle \times \left[1 - \frac{\epsilon_k - \lambda}{E_k}(1 - 2f_k)\right]. \tag{25}$$

The free energy is given by $F = E - \tau S$, where

$$S = -2 \sum_{k>0} [f_k \ln f_k + (1 - f_k) \ln(1 - f_k)] .$$

Since we vary λ so as to keep N fixed the condition $D = \chi Q_0$ gives an extremum in F (Ref. 17) rather than in $F - \lambda N$. If there is more than one self-con-

sistent solution, then the one which gives the minimum value of F should be chosen. Because $N \neq Z$, the actual calculations are more complicated than what is implied in Eq. (17) to Eq. (25). The details can be found in Ref. 16.

The results of such calculations are depicted in Fig. 6. The energies of the various shell model single particle orbitals used for this calculation are given in Table III. The results unfortunately are sensitive to the relative value of g and χ. In Fig. 6 we have shown the results for fixed $g_n = 0.16$ MeV. This gives $\Delta_n = 1.3$ MeV in ^{116}Sn in the spherical zero temperature limit. Since $\Delta_p = 0$, the value of g_p is immaterial. The value of χ lies between the value of Ref. 15 and Ref. 16. Effects of small variations in the value of χ on the free energy curve are shown. We find that shape transition can indeed occur. At zero temperature, the free energy is equivalent to energy and it minimizes at zero deformation. Yet at finite temperature, the free energy may minimize at nonzero deformation,

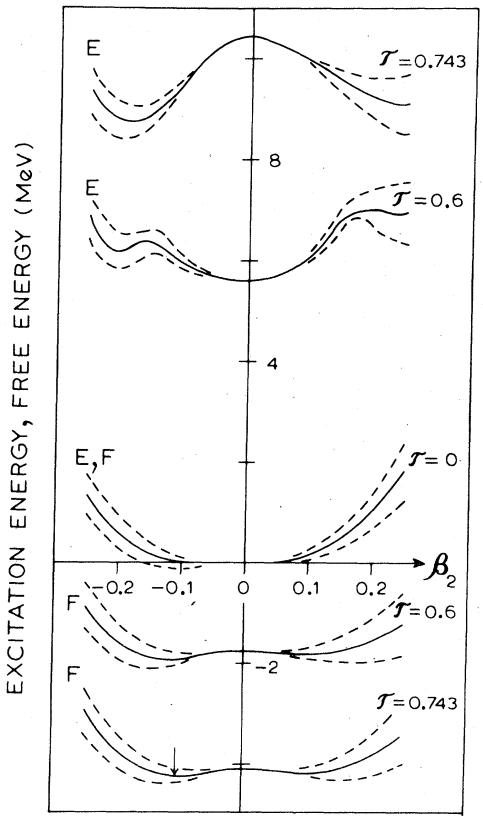

FIG. 6. Potential energy surface and Helmholtz free energy surface as a function of quadrupole deformation for ^{116}Sn at various temperatures τ. The unit of τ is MeV. The solid lines correspond to a quadrupole strength $\chi = 0.0966\ (m\omega/\hbar)^2$ MeV with $\hbar\omega/ = 41.2A^{-1/3}$. The dotted lines give the results for χ altered by ±3%. The arrow indicates the minimum of F for $\tau = 0.743$ MeV.

although the variation of free energy with deformation is not great. If one now takes this deformation as the proper static deformation and performs a standard rotational model calculation for level density, very large differences from the values in Sec. V are found.

Although the free energy against deformation curves are relatively flat, the energy against deformation curves vary more rapidly. They also tend to favor larger deformations.

VII. LEVEL DENSITY USING THE ROTATIONAL MODEL

Since the rotational model formulas are well known,[3,4,17] we merely write down the formulas that were used in the calculation. Assuming a deformation $\beta_2 = -0.104$ (the free energy was minimum at this value of deformation at $\tau = 0.743$ MeV and the corresponding excitation energy was 9.51 MeV) we calculate $\omega_{\text{intr}}(E)$ from which $\rho_{\text{intr}}(E, \Omega)$ is obtained:

$$\rho_{\text{intr}}(E, \Omega) = (2\pi\sigma^2)^{-1/2}\omega_{\text{intr}}(E)e^{-\Omega^2/2\sigma^2}. \tag{26}$$

Here $\rho_{\text{intr}}(E, \Omega)$ is the level density for many-particle states each of which has magnetic quantum number Ω and

$$\sigma^2 = 2\sum_{k>0} k^2 f_k(1 - f_k) \tag{27}$$

In Eq. (27) K is the magnetic quantum number for each Nilsson-type orbital. Now

$$\rho(E, I) = \sum_{\Omega \geq 0}^{I} \rho_{\text{intr}}[E - E_{\text{rot}}(\Omega, I), \Omega] \tag{28}$$

and the rotational model prescribes

$$E_{\text{rot}}(\Omega, I) = \frac{\hbar^2}{2\mathcal{I}_\perp}[I(I+1) - \Omega^2]. \tag{29}$$

Here $\mathcal{I}_\perp$ is the moment of inertia about an axis perpendicular to the symmetry axis. Combining Eqs. (28) and (29) and with the usual approximation one finally obtains

$$\rho(E, I, +) \simeq \tfrac{1}{2}\sum_{\Omega \geq 0}^{I} \rho_{\text{intr}}(E, \Omega) \times \exp\left\{-\frac{\beta\hbar^2}{2\mathcal{I}_\perp}[I(I+1) - \Omega^2]\right\}. \tag{30}$$

The rigid body moment of inertia is used in the calculation. Because only $I = 0$ and 1 are needed to compare with experimental data, the calculated value for level density is insensitive to the choice $\mathcal{I}_\perp$. Reducing $\mathcal{I}_\perp$ by a factor of 2 changes the calculated level density by a few percent.

The method outlined in this section gave

$$\rho(E, 0, +) + \rho(E, 1, +) = 6 \times 10^4\ \text{MeV}^{-1}$$

for ^{116}Sn at the neutron separation energy. The experimental value[18] is 2×10^4 MeV^{-1}. The spherical model (Sec. V) gives 2×10^3 MeV^{-1}. The neutron separation energy in ^{116}Sn is 9.53 MeV. At this energy, with our forces the gap Δ_n has already gone to zero. We know from our model calculation in Secs. II and III (see the last paragraph in Sec. III) that above the gap the grand partition method overestimates the exact level density. Looked at in this light, the deformed model is in much better agreement with experiment than the spherical model.

VIII. DISCUSSION

The present work had two objectives. One was to obtain the exact level density in a semirealistic space when the only interaction is the pairing force. This then allows one to test the validity of various approximate methods that are in current use.

If one considers the quadrupole force in addition to the pairing force, quite interesting features emerge. In the cases investigated, the nucleus is spherical in the ground state, yet it is more proper to think of it as being deformed when considering 8–9 MeV excitations. While this is an idealized model, it is more valid than a simple spherical model for level densities. It will be very interesting to verify if similar results are obtained with more realistic interactions.

We wish to thank Professor N. B. de Takacsy for several useful discussions.

---

*National Research Council of Canada Fellow.

†Work supported by the Canadian Commonwealth Scholarship and Fellowship Program.

[1]P. Decowski, W. Grochulski, A. Marcinkowski, K. Siwek, and Z. Wilhelmi, Nucl. Phys. A110, 129 (1968).

[2]L. G. Moretto, Nucl. Phys. A185, 149 (1972).

[3]T. Dossing and A. S. Jensen, Nucl. Phys. A222, 145 (1972).

[4]J. R. Huizenga, A. N. Bekhami, J. S. Sventek, and R. W. Atcher, Nucl. Phys. A223, 577 (1974); J. R. Huizenga, A. N. Bekhami, R. W. Atcher, J. S. Sventek, H. C. Britt, and H. Freiesleben, *ibid.* A223, 589 (1974).

[5]L. A. Malov, V. G. Soloviev, and V. V. Vononov, Nucl. Phys. A224, 396 (1974); V. G. Soloviev, Ch. Stoyanov, and A. I. Vdovin, *ibid.* A224, 411 (1974).

[6]F. N. Choudhury and S. Das Gupta, Phys. Rev. C 16, 757 (1977).

[7]S. Kahana, H. C. Lee, and C. K. Scott, Phys. Rev. 180, 956 (1969).

[8]L. S. Kisslinger and R. A. Sorensen, Rev. Mod. Phys. 35, 853 (1963).

[9]A. Kerman, Ann. Phys. (N. Y.) 12, 300 (1961); A. Kerman, R. D. Lawson, and M. H. Macfarlane, Phys. Rev. 124, 162 (1961).

[10]J. B. French, in *Nuclear Structure*, edited by A. Hossain, Harun-ar-Raschid, and M. Islam (North-Holland, Amsterdam, 1967), p. 85; F. S. Chang, J. B. French, and T. H. Thio, Ann. Phys. (N. Y.) 66, 137 (1971).

[11]S. Das Gupta and R. K. Bhaduri, Phys. Lett. 58B, 381 (1975).

[12]W. Y. Ng and S. S. M. Wong, Can J. Phys. 54, 2287 (1976).

[13]I. Kanestrom, Nucl. Phys. 83, 380 (1966).

[14]M. Hillman, Phys. Rev. C 9, 2289 (1974).

[15]Krishna Kumar and Michel Baranger, Phys. Rev. Lett. 12, 73 (1964).

[16]M. Baranger and K. Kumar, Nucl. Phys. A110, 490 (1968).

[17]N. H. March, W. H. Young, and S. Sampanthar, *The Many-Body Problem in Quantum Mechanics* (Cambridge Univ. Press, Cambridge, 1967), p. 243.

[18]H. Baba, Nucl. Phys. A159, 625 (1970).